A Theory of Rotating Stall of Multistage Axial Compressors: Part I—Small Disturbances[1]

F. K. Moore
Sibley School of Mechanical and Aerospace Engineering, Cornell University, Ithaca, N.Y. 14853

An analysis is made of rotating stall in compressors of many stages, finding conditions under which a flow distortion can occur which is steady in a traveling reference frame, even though upstream total and downstream static pressure are constant. In the compressor, a pressure-rise hysteresis is assumed. Flow in entrance and exit ducts yield additional lags. These lags balance to give a formula for stall propagation speed. For small disturbances, it is required that the compressor characteristics be flat in the neighborhood of average flow coefficient. Results are compared with the experiments of Day and Cumpsty. If a compressor lag of about twice that due only to fluid inertia is used, predicted propagation speeds agree almost exactly with experimental values, taking into account changes of number of stages, stagger angle, row spacing, and number of stall zones. The agreement obtained gives encouragement for the extension of the theory to account for large amplitudes.

Introduction

In recent years, experimental studies and reviews by Greitzer, Day, and Cumpsty [1, 2, 3] have clarified and redefined the problem of rotating stall of axial flow compressors, giving a new emphasis to the compressor of many stages. At low flows, virtually all compressors exhibit zones of stalled flow which propagate tangentially, with blade passages cyclically stalling and recovering in the manner first described by Emmons [4].

However, when the compressor has many stages (about three seems to suffice), the stall patterns seem to be simpler and presumably more predictable than when the compressor consists of a single row or stage. Early reviews [5] convey this impression, but it remained for Day, Greitzer, and Cumpsty [3] to describe what one might call the kinematics of rotating stall. They demonstrated, for example, that the stall pattern in "deep stall" tends to run straight through the machine, with an especially abrupt transition at the trailing edge of the stall zone.

Theoretical studies in the past [6–9] have attempted to understand rotating stall for a single stage under the natural impression that if one could properly relate the Emmons type of stalling-unstalling episodes to the individual cascade characteristics, then one could proceed to synthesize a theory for multistage machines. This approach, though logical, has not been fruitful. In effect, rotating stall is too universal a phenomenon and depends on too many variables; single-stage analysis does not yield critical conditions meaningful for whole-compressor performance, especially in deep stall.

In the present three-part study, we explore the idea that rotating stall theory should begin with the compressor of many stages, operating in stall. Doing this, we will not emphasize the problem of "stall inception," but, rather, try to incorporate in the theory the kinematic features of deep stall described by Day, Cumpsty, and Greitzer [3]. Greitzer and Cumpsty [10] have presented a semiempirical analysis of deep-stall propagation speed which is in this same spirit.

In this paper (Part I), a single dynamic hysteresis is assumed for the blade-passage force function and conditions are derived for the occurrence of a weak stall pattern which is steady in some rotating frame of reference. From this analysis we find a formula for stall propagation speed which agrees well with experimental data, if the single lag parameter is properly chosen.

In Part II, the analysis is extended to describe the stall patterns of arbitrary velocity amplitude which can occur when the quasi-steady compressor characteristic is either flat (deep stall) or else curved as it would be at stall inception. Wave forms for velocities and pressure are found, as well as propagation speeds and the distortion of the compressor characteristic due to rotating stall.

In Part III, a compressor characteristic is adopted which has the realistic feature of an unstalled region with peak pressure rise, a deep-stall valley, and a steep resistance to reversed flow. Rotating stall then is found to have the nature of a limit cycle, familiar in the classical van der Pol problem of nonlinear mechanics [11]. Results include a prediction of stall recovery as flow coefficient is increased.

The present paper, though limited in results to weak disturbances, will include certain developments in forms suitable for more general application in subsequent parts.

Support for this work by NASA-Lewis during the author's sabbatic leave from Cornell is gratefully acknowledged, as

[1] Research performed at NASA-Lewis Research Center, Cleveland, Ohio

Contributed by the Gas Turbine Division of THE AMERICAN SOCIETY OF MECHANICAL ENGINEERS and presented at the 28th International Gas Turbine Conference and Exhibit, Phoenix, Arizona, March 27–31, 1983. Manuscript received at ASME Headquarters, December 20, 1982. Paper No. 83-GT-44.

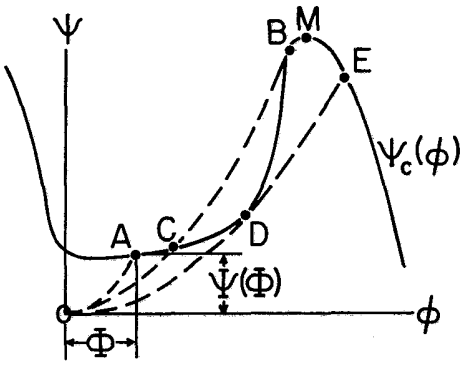

Fig. 1 Constant-speed compressor characteristic, $\psi_c(\phi)$, and operating points, $\Psi(\Phi)$; upstream total to downstream static pressure rise versus axial flow coefficent

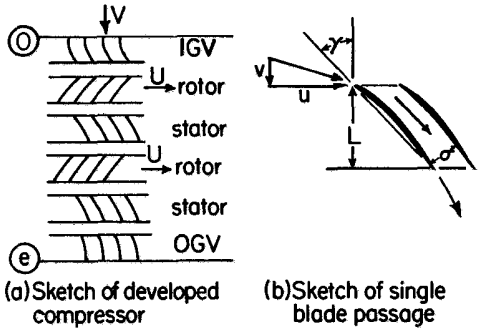

Fig. 2 Sketch of compressor configuration. Number of stages is arbitrary; two are shown. Radial effects are neglected. Entrance and exit planes are denoted by ⓞ and ⓔ. Blading is symmetrical.

well as helpful discussions with C. L. Ball, Lonnie Reid, and M. E. Goldstein in the course of the study.

The Compressor

The compressor is assumed to have a constant-speed characteristic as sketched in the solid line of Fig. 1. We will denote the upstream total (p_T) to downstream static (p_s) pressure-rise coefficient by ψ_c, in the absence of rotating stall

$$\frac{p_s - p_T}{\rho U^2} \equiv \psi_c(\phi) \tag{1}$$

The axial flow coefficient, ϕ, has the average value, Φ

$$\frac{v}{U} \equiv \phi; \quad \frac{V}{U} \equiv \Phi. \tag{2}$$

The characteristic ψ_c will be considered to be single-valued, as shown. Throttle settings, indicated by dashed parabolic lines, will intersect the characteristic and establish operating points (A–E on the sketch) about which rotating stall might occur. Points B and D in the sketch would indicate limits of a quasi-steady hysteresis loop (B – C – D – E) due (we assume) purely to the way the throttle parabolas intersect the characteristic. In Parts II and III, we shall permit the net pressure rise (Ψ) to depend on the existence of rotating stall. For example, the operating point in rotating stall for the Φ indicated at point A might actually lie above or below the characteristic curve.

The compressor has N stages, with IGV and OGV rows providing zero incidence at design. Blading and design vector diagrams are symmetrical (50 percent reaction) as sketched in Fig. 2. Radial effects will be neglected, and flow will be considered incompressible.

Flow Disturbance in the Compressor

First, a disturbance will be postulated to exist in the compressor, steady in a circumferentially moving frame. This disturbance implies disturbances in the flow fields entering and leaving the compressor. The plan of this study is to find the requirement that such a set of disturbances exists, even though pressures far upstream and downstream remain constant; in effect, to find eigensolutions and eigenvalues for the whole system. We begin by describing the disturbance of a single blade passage.

Disturbance in a Blade Passage. When rotating stall occurs flow velocities will change locally and in time. We will assume that when axial flow is slowly reduced, keeping U constant, flow fields of rotor and stators remain symmetrical, though pressure rise and deviation should change. In other words, the quasi-steady velocity triangles remain symmetrical, and corresponding pressure changes are equal. Pressure rise in each row is assumed to depart slightly from the quasi-steady, however.

The static pressure rise through each row will be assumed to have the form

$$\frac{\Delta p}{\frac{1}{2}\rho U^2} = F(\phi) - \tau(\phi)\dot{\phi} \tag{3}$$

whether rotor or stator.

The quasi-steady pressure-rise coefficient, F, might have

Nomenclature

a_n, b_n = Fourier coefficient of $g(\theta)$, equation (18a)
D = mean wheel diameter
F = steady pressure rise coefficient in blade passage, equation (3)
f = stall propagation-speed coefficient, equation (11) and Fig. 4
g = axial flow coefficient perturbation in compressor, equation (4)
h = transverse velocity coefficient perturbation at entrance, equation (15)
K_I = pressure-rise parameter at IGV entrance, equation (8)
k = parameter relating actual compressor-row lag to interia lag of blade passage only
L = depth of row in axial direction, Fig. 2(b)
m = parameter defining lag tendency outside compressor, equation (34)
N = number of stages in compressor core
n = wave number, corresponding to number of stall cells
P = pressure coefficient, equation (24)
p = static pressure
U = wheel speed at mean wheel diameter
u = transverse velocity in laboratory frame
V = average axial velocity
v = axial velocity
x = circumferential distance, in stall-zone frame, equation (5)
y = distance normal to compressor face, in flow direction, Figs. 4, 5
γ = stagger angle of blades, Fig. 2

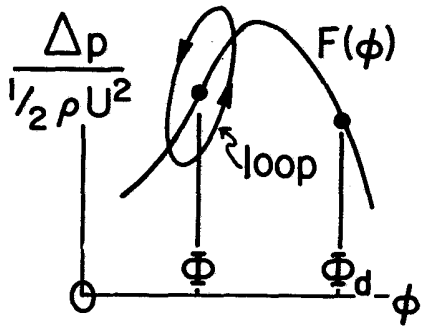

Fig. 3 Assumed form of blade-passage pressure-rise function

the form sketched in Fig. 3. Assigning the same F to each row, and properly taking account of dynamic pressure, $F(\phi)$ will yield the ψ_c of Fig. 1. The occurrence of a maximum of F, and the drop of F as ϕ is reduced, will signify stall of a blade passage.

The second term describes hysteresis due either to flow acceleration, flow separation, or viscous processes in the blade passage. It is written in the sense that if ϕ is decreasing, then there is an extra force which is positive. At any flow coefficient, therefore, we assume a counterclockwise dynamic hysteresis loop, as sketched in Fig. 4. The parameter, τ, will generally be a function of ϕ, of course. However, throughout this study, we will take τ to be constant, and the same for rotors and stators.

Because equation (3) will be considered to apply equally to the rotor and stator rows, in effect we disregard centrifugal and secondary-flow phenomena. In fact, for symmetric blading, τ would be the same for rotors and stators. For guide vanes, we will adopt the same equation, using subscripts to distinguish them from the stage elements.

Stall Pattern of the Compressor. If, by symmetry, rotor and stator blade passages show no deviation under disturbance, and no flow development takes place between rows (as if there is zero inter-row spacing), then continuity will require that all instantaneously connected blade passages have the same axial velocity. Therefore, any disturbance of axial velocity would be purely circumferential, however many stages there are, and whatever the speed of propagation of the disturbance pattern. Further study might show that dynamic effects will require modification of this symmetry argument.

Under present assumptions, a stall pattern, shown shaded on Fig. 4, must proceed straight through the machine. This is consistent with observations of deep stall. Obviously, if reaction is not 50 percent or blades are of unequal axial

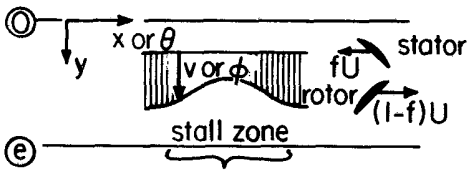

Fig. 4 Sketch showing axial stall zone in compressor, in coordinates fixed in the stall zone which, in laboratory coordinates, is moving to the right at speed, fU

length, if compressibility or centrifugal effects were significant, or if circumferential flow between rows is allowed, then the straight-through pattern would not be correct.

Next we assume that a disturbance pattern is steady in some rotating frame of reference. If the compressor is "unwrapped" as in Fig. 4, the disturbance is moving to the right with speed fU relative to stators. The "stall propagation speed" f is unknown; it is to be found as an eigenvalue of the disturbance, so to speak. Relative to the disturbance, stators are moving to the left with speed fU and rotors are therefore moving to the right with speed $(1-f)U$. The axial flow coefficient in this frame takes the form

$$\phi=\Phi+g(\theta) \tag{4}$$

where g represents a steady disturbance. Again referring to Fig. 4, distance x is measured to the right, so that

$$\theta=2x/D \tag{5}$$

where D is the mean diameter of the compressor. If the disturbance of ϕ is purely circumferential, then equation (3) applies equally to each blade row, and pressure-rise may be accumulated through the compressor purely as a function of θ, or equivalently, x.

The time derivative, $\dot{\phi}$, must be expressed in terms of the steady disturbance described in equation (4) and Fig. 4; it signifies the rate of increase of ϕ experienced by a blade passage as it traverses the postulated stall disturbance. Thus from equations (4) and (5)

$$\dot{\phi}=g'(\theta)\dot{\theta}=g'(\theta)\frac{2\dot{x}}{D} \tag{6}$$

Figure 4 sketches the situation: The solid line represents the steady but disturbed flow, $\phi(\theta)$. Stator blades moving to the left at speed fU experience an increase of ϕ depending on the local gradient of ϕ (that is, $\phi'(\theta)$) and the relative speed $\dot{x}=-fU$. Similarly, a rotor moves in the same gradient with speed $\dot{x}=(1-f)U$. For stators and rotors separately

Nomenclature (cont.)

ϵ = amplitude parameter of disturbance, equation (19)
θ = angular location, in stall-zone frame, equation (5)
λ = collection of terms analogous to oscillator mass, equation (39)
ρ = density
σ = normal blade passage width, Fig. 2(*b*)
τ^* = reduced time lag, equation (45)
τ = coefficient of pressure-rise hysteresis, equation (3)
Φ = average flow coefficient, V/U
ϕ = flow coefficient, v/U
$\tilde{\phi}$ = velocity potential, equation (13)
Ψ = upstream total to downstream static pressure-rise coefficient existing during operation
ψ_c = compressor characteristic in absence of rotating stall, Fig. 1
$\tilde{\psi}$ = stream function, equation (23)

Superscripts

• = time derivative
= = ordinary differentiation

Subscripts

d = design conditions
e = at compressor exit
IV = inlet guide vane
OV = outlet guide vane
s = far downstream static conditions
T = far upstream total conditions
0 = just ahead of compressor entrance
∞ = far upstream static conditions

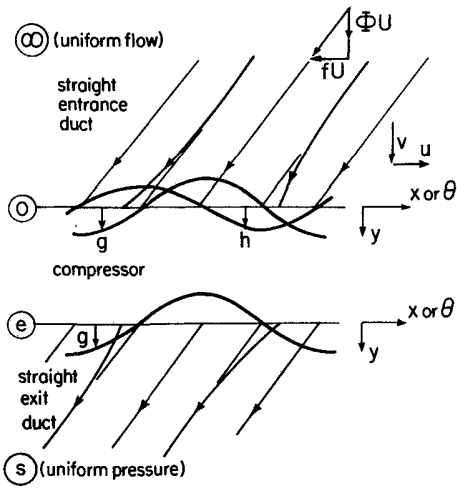

Fig. 5 Sketches of flows in straight entrance and exit ducts, coordinates fixed in disturbance. At the compressor exit, $u = -fU$.

$$\dot{\phi}_{\text{stator}} = -g'(\theta)\frac{2U}{D}f \tag{7a}$$

$$\dot{\phi}_{\text{rotor}} = g'(\theta)\frac{2U}{D}(1-f) \tag{7b}$$

Since it is intended to accumulate forces through the compressor, we will find use for the combined pressure-rise expression for a single stage

$$\left(\frac{\Delta p}{\frac{1}{2}\rho U^2}\right)_{\text{stage}} = 2F(\phi) - \tau g'(\theta)\frac{4U}{D}\left(\frac{1}{2}-f\right) \tag{8}$$

Guide Vanes. The OGV is assumed to have no deviation, and will therefore deliver flow in a purely axial direction to the diffuser. A hysteresis term (equation (3)) applies with a value of τ_{OV} presumably different from the τ applicable to stators and rotors of the stages.

It will be assumed that IGV's are purely axial at entrance. When rotating stall occurs, there will be (as we shall find) a transverse velocity disturbance at the compressor (IGV) entrance. In this paper, we will consider this velocity disturbance small compared to V. Regarding the IGV as a nozzle, its entering velocity will therefore depart from the local value of v only to second order in small quantities. Accordingly, although there must be a rather abrupt pressure rise crossing the entrance plane of the IGV's, it too will be of second order in flow deflection. By our previous stage symmetry argument, we should expect the IGV discharge angle to be the same as the OGV entrance angle. Thus, recalling equation (3), there should be negative value of F for the IGV nozzle, just equal to the positive value for the OGV passage acting as a diffuser, even though ϕ varies. Again a hysteresis term should apply, and, for OGV and IGV together, one has, corresponding to equation (8),

$$\left(\frac{\Delta p}{\frac{1}{2}\rho U^2}\right)_{\substack{\text{guide}\\ \text{vanes}}} (\tau_{IV}+\tau_{OV})g'(\theta)\frac{2U}{D}f + K_I h^2 \tag{9}$$

where $K_I h^2$ represents the coefficient of abrupt pressure rise at the IGV entrance.

Upstream Disturbance

Far upstream, we imagine a reservoir of total pressure, p_T, constant whether or not rotating stall is in progress. Between that reservoir and the compressor face is a flow passage of some possibly complex shape ("Gooseneck"). In that region, a flow disturbance will develop, if rotating stall exists. In this study, we shall assume the entrance region to be a straight, uniform channel. In that case, if the flow upstream has uniform velocity and pressure

$$p_\infty = p_T - \frac{1}{2}\rho V^2 \tag{10}$$

and V will be the average velocity of any disturbance that arises downstream.

Velocity Field. In the channel, disturbances will be considered irrotational as well as incompressible. Thus, Laplace's equation applies. For convenience, we adopt the coordinate system of Fig. 4, so that the velocity components far upstream ($y = -\infty$) are

$$\frac{u_\infty}{U} = -f; \quad \frac{v_\infty}{U} = \frac{V}{U} \equiv \Phi \tag{11}$$

At the compressor face, equation (4) applies

$$\frac{v}{U} = \phi = \Phi + g(x) \tag{12}$$

The resulting steady streamline pattern in the entrance duct region will be as sketched in Fig. 5. It will be necessary to know the pressure disturbance at the compressor face, and, for this, the value of u there is needed. We may write a disturbance velocity potential

$$\frac{u}{U} = -f + \tilde{\phi}_x; \quad \frac{v}{U} = \Phi + \tilde{\phi}_y \tag{13}$$

with $\tilde{\phi}$ vanishing when $y = -\infty$, and at $y = 0$

$$(\tilde{\phi}_y)_0 = g(\theta) \tag{14}$$

where g is arbitrary but periodic, with wavelength $\pi D/n$. The wave number, n, is introduced to account for the possibility of multiple-cell stall. The required u-velocity at the compressor face will henceforth be designated as $h(x)$

$$(\tilde{\phi}_x)_0 = h(\theta) \tag{15}$$

In general, h is the Hilbert transform of g

$$h(\theta) = -\frac{1}{\pi}\int_{-\infty}^{\infty}\frac{g(\xi)d\xi}{\theta-\xi} \tag{16}$$

Takata and Nagano [9] integrated this relation numerically for certain unsteady disturbances. If g is periodic, it may be shown that equation (16) yields

$$h = -\frac{1}{\pi}\int_0^{2\pi} g'(\xi)\ln\left|\sin\frac{\theta-\xi}{2}\right| d\xi \tag{17}$$

If $g(\theta)$ has a Fourier series

$$g(\theta) = \sum_1^\infty (a_n \sin n\theta + b_n \cos n\theta) \tag{18a}$$

then

$$\tilde{\phi}(y,\theta) = \sum_1^\infty \frac{D}{2n} e^{n\frac{2y}{D}}(a_n \sin n\theta + b_n \cos n\theta) \tag{18b}$$

which satisfies equation (14) and vanishes at $y = -\infty$. The corresponding u and v velocities both vanish as they should at $y = -\infty$, and

$$h(\theta) = \sum_1^\infty (a_n \cos n\theta - b_n \sin n\theta) \tag{18c}$$

For example, if g is a harmonic wave

$$g = \epsilon\Phi \sin n\theta; \quad h = \epsilon\Phi \cos n\theta \tag{19}$$

ϵ being an amplitude parameter.

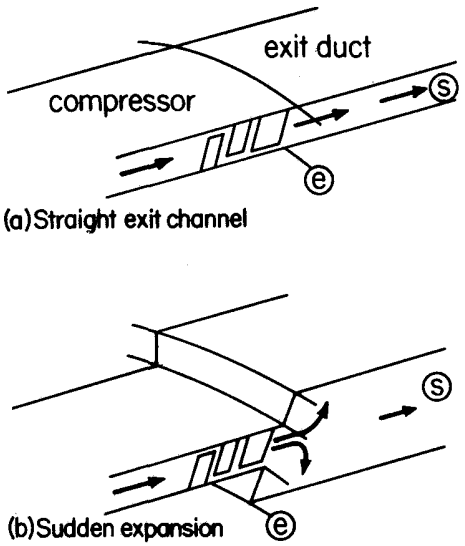

Fig. 6 Sketches of extreme exit-duct configuration

Pressure Field. In the disturbance coordinates, the steady Bernoulli equation applies

$$p_\infty + \frac{1}{2}\rho U^2(f^2+\Phi^2) = p_0 + \frac{1}{2}\rho U^2[(-f+h)^2+(\Phi+g)^2] \quad (20)$$

where p_0 is the pressure at the compressor face, just ahead of the IGV. Recalling equation (10), one finds

$$\frac{p_0-p_T}{\rho U^2} = -\left(\frac{1}{2}\Phi^2+\Phi g+\frac{1}{2}g^2-fh+\frac{1}{2}h^2\right) \quad (21)$$

If g is a weak harmonic wave, equation (19), with ϵ assumed small compared to 1, would provide

$$\frac{p_0-p_I}{\rho U^2} = -\frac{1}{2}\Phi^2 - \epsilon(\Phi^2 \sin n\theta - f\Phi\cos n\theta) \quad (22)$$

to first order in ϵ.

If the channel is not straight, or if the flow in the channel is not irrotational, equations (21) and (22) would require modification.

Downstream Disturbance

Far downstream, we imagine a flow of uniform static pressure (p_s), but no necessarily constant velocity; a shear flow might be the final result. The flow is expected to emerge from the OGV in an axial direction (viewed in stator coordinates) but with varying pressure (p_e) and perhaps vorticity. The actual exit-flow device, or diffuser, is very important in this regard, and we will limit this discussion to two types, a straight channel, and a sudden expansion. These two extreme types perhaps bracket the possibilities.

Straight Channel. If there is a straight, constant-area channel downstream of the compressor exit (Fig. 6(a)) then the Euler equations must be solved in the region sketched in Fig. 5. Defining a stream function for that region

$$\frac{u}{U} = \tilde{\psi}_y; \quad \frac{v}{U} = \phi = -\tilde{\psi}_x \quad (23)$$

and expressing pressure in the dimensionless form

$$\frac{p_s-p}{\rho U^2} \equiv P \quad (24)$$

where p_s is the (constant) downstream static pressure, one may write the Euler equations as

$$-P_x = -\tilde{\psi}_y\tilde{\psi}_{xy} + \tilde{\psi}_x\tilde{\psi}_{yy}; \quad -P_y = \tilde{\psi}_y\tilde{\psi}_{xx} - \tilde{\psi}_x\tilde{\psi}_{xy} \quad (25)$$

Boundary conditions at the rear face of the compressor (subscript e) at $y=0$ are

$$(\tilde{\psi}_y)_e = -f; -(\tilde{\psi}_x)_e = \Phi + g(x) \quad (26)$$

and far downstream (subscript s) at $y=\infty$, the pressure must become uniform, but vortical velocity disturbances may survive

$$P_s = 0 \quad (27)$$

In formulating a solution of the system of equations (25-27), we should recall that only P is needed, in its relation to the disturbance function $g(x)$. Equation (25) can be converted to

$$\frac{1}{2}\nabla^2 P = -\tilde{\psi}_{xx}\tilde{\psi}_{yy} + (\tilde{\psi}_{xy})^2 \quad (28)$$

and equations (25) and (26) yield

$$(P_y)_e = -fg'(x) \quad (29)$$

Of course, one or the other of equation (25) must be included with equation (28). However, if the disturbance is weak, then the right side of equation (28) is of second order, and equation (28) is simply Laplace's equation

$$\nabla^2 P = 0 \quad (30)$$

The desired solution for P can be found directly, using equations (27) and (29) as boundary conditions.

In fact, the function $-P/f$ would correspond to the x-derivative of a velocity potential, vanishing at $y=\infty$, of which $g(x)$ is the y-derivative at $y=0$. But that is precisely the relationship between g and h defined in equations (14) and (15). Taking account of the difference of direction of y between the two cases, one may immediately conclude that

$$P_e = fh; \quad P_e \equiv \frac{p_s-p_e}{\rho U^2} \quad (31)$$

This is not a general result, because the right side of equation (28) was set equal to zero. It is, however, correct to first order in small quantities if, for example, equation (19) applies, and may be a useful relation even if disturbances are not weak.

If disturbances are indeed weak, equations (25) and (31) may be used to find the velocity field in the straight channel. The result for $\tilde{\psi}$ is

$$\tilde{\psi} = \frac{D}{2n}\left\{-\Phi n\left(\theta+2\frac{f}{\Phi}\frac{y}{D}\right) + \epsilon\frac{\Phi^2}{\Phi^2+f^2}\left[f\sin n\left(\theta+2\frac{f}{\Phi}\frac{y}{D}\right) + \Phi\cos n\left(\theta+2\frac{f}{\Phi}\frac{y}{D}\right) + \frac{f}{\Phi}e^{-2n\frac{y}{D}}(-\Phi\sin n\theta + f\cos n\theta)\right]\right\} \quad (32)$$

If disturbances are of finite strength, and if $g(\theta)$ can be expressed as a Taylor series in ϵ, then the full equation (28) could be made the basis of a method of successive approximations.

Sudden Expansion. If there is a sudden large transverse (radial) expansion just at the OGV exit, as sketched in Fig. 6(b), then the exit flow would be like a jet emerging from a long slot. While the jet velocity would vary circumferentially on a scale comparable to wheel diameter, the pressure matching of the jet to the receiver would occur on the scale of blade height. Since the receiver pressure could be considered constant, the jet exit pressure could also be considered constant. In the extreme of an orifice-like diffuser

$$p_e = p_s \quad (33)$$

This is the simplest possible assumption about pressure change at the compressor exit [9]. Of course, it envisages an extremely short diffuser, which would generally not be acceptable because of its low efficiency.

Apparently, the general problem of finding the pressure change at the compressor exit is quite difficult, both to define and to solve. The specifics of diffuser configuration would greatly affect the result. Here, we have found expressions for two extreme cases which may possibly bracket typical practical situations. We may, for convenience, write them in the form

$$P_e = \frac{p_s - p_e}{\rho U^2} = (m-1)fh \tag{34}$$

where $m=1$ would signify a sudden area change, and $m=2$ would signify a straight channel. We will regard m, therefore, as a somewhat arbitrary parameter of our problem.

Requirements for Rotating Stall

The various pressure relations may now be combined to express a statement that pressures remain constant in upstream and downstream reservoirs, even though an unsteady disturbance occurs in the compressor which connects them. We have already specified that the disturbance is steady when viewed in a frame rotating with velocity, fU.

Pressure Match. We require that $p_s - p_T$ be constant, or

$$\underbrace{\frac{p_0 - p_T}{\rho U^2}}_{\text{entrance duct}} + \underbrace{\frac{p_e - p_0}{\rho U^2}}_{\text{compressor}} + \underbrace{\frac{p_s - p_e}{\rho U^2}}_{\text{exit duct}} = \underbrace{\frac{p_s - p_T}{\rho U^2}}_{\text{reservoirs}} \equiv \Psi \tag{35}$$

The first term is given by equation (21), the third by equation (34), and the second by application of equation (9) for guide vanes and equation (8) for each of N stages. The result may be written

$$\left[\frac{2UN\tau}{D}\left(\frac{1}{2}-f\right) - \frac{U(\tau_{IV}+\tau_{OV})}{D} f\right] g'(\theta) - mfh + \frac{1}{2}h^2 - \frac{1}{2}K_I h^2 + \Psi - \left[NF(\phi) - \frac{1}{2}\phi^2\right] = 0 \tag{36}$$

It is obvious that the last quantity in brackets is the compressor characteristic function that would apply in the absence of rotating stall; that is, the curve $\psi_c(\phi)$ shown on Fig. 1.

$$\psi_c(\phi) \equiv NF(\phi) - \frac{1}{2}\phi^2 \tag{37}$$

It should be emphasized that while $\psi_c(\phi)$ is a given feature of the compressor, it is not the same as Ψ; the latter is the pressure rise actually produced, with rotating stall (if it occurs) in progress. While ψ_c is, in principle, given, it is not the characteristic usually measured in tests of compressors subject to rotating stall. One might rather say that Ψ is the usually measured quantity; here, it is part of the answer.

The problem now is to find what values of parameters such as f, m, Ψ, or features of the function $\psi_c(\phi)$, permit nonzero solutions of the pair of equations (36) and (17).

Weak Disturbances. In this paper, we will restrict disturbances to be weak. Thus, we neglect the terms $(1/2)h^2$ and $(1/2)K_I h^2$ appearing in equation (36). Also, since ϕ will remain close to Φ during a weak disturbance, we keep only the first two terms of the Taylor series

$$\psi_c(\phi) = \psi_c(\Phi) + \psi_c'(\Phi)g + \frac{1}{2}\psi_c''(\Phi)g^2 + \ldots \tag{38}$$

For convenience, we define

$$\lambda \equiv \frac{2UN\tau}{D}\left(\frac{1}{2}-f\right) - \frac{U(\tau_{IV}+\tau_{OV})}{D} f \tag{39}$$

so that equation (36) becomes

$$\lambda g'(\theta) - mfh - \psi_c' g + \Psi - \psi_c(\Phi) = 0 \tag{40}$$

By definition, the average value of g over a cycle must vanish. Also, if the flow far upstream is purely axial, no average swirl can arise between there and the compressor entrance if the flow is irrotational. Therefore, the average value of h must also vanish. These conditions would apply even for strong waves, but in the present case, integrating equation (40) over a cycle shows that

$$\Psi - \psi_c(C) = 0 \tag{41}$$

In other words, for weak waves, there is no vertical displacement of the operating point from the rotating-stall-free characteristics; it is as indicated for point A of Fig. 1.

Presumably, g and h have Fourier series with coefficients related by equations (18(a) and 18(c)). Because equation (40) is linear, each coefficient is independently fixed. Using only the a_n terms, we find by substitution

$$(\lambda n - mf)a_n \cos n\theta - \psi'(\Phi)a_n \sin n\theta = 0 \tag{42}$$

The conditions for a weak periodic wave of arbitrary amplitude are therefore that $\lambda n = mf$, that $\psi_c'(\Phi) = 0$, and that $\Psi = \psi_c(\Phi)$. The first of these may be solved for propagation-speed coefficient, f

$$f = \frac{1/2}{1 + m\dfrac{D}{2UnN\tau} + \dfrac{\frac{1}{2}(\tau_{IV}+\tau_{OV})}{N\tau}} \tag{43}$$

This is the chief result of our analysis, and will be discussed fully in the next section. The second requirement

$$\psi_c'(\Phi) = 0 \tag{44}$$

means that the local curve of ψ_c must be flat. This could be true in the deep-stall region (points like A or C in Fig. 1), and is true at the maximum of the characteristic (point M). In the latter case, equation (44) would be a conditon for stall inception, agreeing with the classical stability requirement. On the descending branch of the speed line, equation (44) would not be satisfied; we interpret that to mean not that rotating stall cannot occur, but rather that it cannot be weak. In fact, ψ_c' can be interpreted as a negative damping factor; since equations (18) indicate that $g = -h'$, equation (40) is that of a harmonic oscillator,

$$\lambda h'' - \psi_c' h' + mfh = 0$$

with homogeneous boundary conditions, a wave must decay if ψ_c' is negative, or be amplified if ψ_c' is positive. In neither case could a permanent oscillation exist.

Equations (41), (43), and (44) therefore give the conditions for a steady rotating stall of weak amplitude to exist, when reservoir pressures are both constant.

Stall Propagation Speed

We next discuss the implications of equation (41) and compare its predictions with experiment [2]. Equation (43) is essentially a balance of disturbance phase lags inside and outside the compressor.

The External Lag Parameter. The parameter, m, appears in equation (43). It was defined in equation (34) as a measure of the strength of the lagging pressure term fh arising in the exit duct. The same lag term arises from the entrance duct (the term fh in equation (21)) assuming ideal flow in a straight

channel. We should admit the possibility that in the entrance flow, too, configuration or loss effects might affect lag. Thus, where the two lags are added to give mfh in equation (36), we should imagine m to be a net lag parameter depending on the combined contributions of both entrance and exit flows.

The Compressor Lag Parameters. The lag, τ, defined in equation (3), depends on the aerodynamics of a blade passage, sketched in Fig. 2(*b*). Whatever its physical nature, it should scale with axial passage length, L, and axial velocity, V. We are then led to define a dimensionless lag

$$\tau^* \equiv \frac{\Phi U \tau}{L} \tag{45}$$

in terms of which equation (43) becomes

$$f = \frac{1/2}{1 + \frac{m\Phi}{n}\frac{D}{2NL}\frac{1}{\tau^*} + \frac{1}{N}\frac{\tau_v^*}{\tau^*}} \tag{46}$$

The lags for guide vanes are assumed equal.

It is perhaps of interest to note the value of τ^* that would represent "apparent mass" or inertia only. Referring to Fig. 2(*b*), we see that a mass $\rho L\sigma/\cos\gamma$ of fluid is accelerating in a blade passage at a rate $U\dot{\phi}/\cos\gamma$ requiring the force provided by an additional pressure rise $(\Delta p)_A$

$$\frac{(\Delta p)_A}{\frac{1}{2}\rho U^2} = -\frac{2}{\cos^2\gamma}\frac{L}{U}\dot{\phi} \tag{47}$$

Comparing equation (3) we see that, due to inertia in blade passages only, $\tau^* = 2\Phi/\cos^2\gamma$. The stagger angle, γ, is roughly $\tan^{-1}(1/2\ \Phi_d)$ where Φ_d is design flow coefficient. We write

$$\tau^* = \frac{2\Phi}{\cos^2\gamma}k \tag{48}$$

where a factor k has been included because, often, the interrow gap is quite large. If the gap were a multiple $k-1$ of L, then τ^* would be proportional to k.

Other effects having to do with separation or secondary flows will also influence τ^*. If these could be represented by suitable choice of k, it would be appropriate to write equation (46) in the following form

$$f = \frac{1/2}{1 + \frac{m}{k}(\cos^2\gamma)\frac{1}{2n}\frac{D}{2NL} + \frac{\tau_v^*}{\tau^*}\frac{1}{N}} \tag{49}$$

We will use k as a general "uncertainty factor" comparing actual τ to blade-passage inertia lag. It is interesting that the external and internal lag parameters enter equation (49) only in their ratio, m/k.

Qualitative Results for Propagation Speed. Equation (46) shows certain general trends:

1 Propagation speed is less than 50 percent of U, unless τ is negative. Actually, negative lag has been argued to occur at stall of isolated airfoils [12], and $f > 1/2$ is generally associated with single-stage experiments [2, 5]. Perhaps these results are consistent.

2 Increasing number of stages (N) increases f toward 1/2. This result has been found by Cumpsty and Greitzer [10]. It is important that N multiplies τ^* in equation (1.46). If τ is very small, being proportional to blade chord, it might at first be thought to make a negligible contribution to pressure rise (equation (3)), and therefore not be proper to include in a disturbance analysis. This argument might be valid for single-row problems. However, a small lag per row will accumulate over many rows in a multistage compressor to make a large overall lag; it is the latter which governs rotating stall. The same idea is expressed by noting the group $D/2NL$ in equation (49); it describes the shape factor of the whole compressor when viewed from the side. Typically it would be of order 1, while for a single row, D/L would be much larger—typically about 15.

Table 1 Propagation speed coefficient

Φ_d	γ (deg)	N	n	Ref. [2]	f (percent) Equation (49) $k/m=1$	f (percent) Equation (49) $k/m=2$
0.35	50	1	1	19	11	16
			6	31	23	26
			12	66	26	27
0.35	50	3	1	32	23	29
			4	40	34	37
			12	60	38	39
0.35 (reducing spacing)	50	3	1	27	23	29
			5	54	35	38
0.55	35	1	1	15	9	14
		2	1	22	15	21
		3	1	26	20	26
		4	1	31	23	30
1.00	20	1	1	11	8	12
		2	1	20	14	20
		3	1	24	18	25
		4	1	28	22	28

Chord = 17.8 mm
Mean diameter: 320 mm

3 Multicell stalls have higher propagation speeds. The mode number, n, represents number of stall cells.

4 Increased lag (larger k) tends to increase propagation speed.

5 Especially if design flow coefficient, Φ_d, is small, smaller Φ_d (or larger stagger angle) will increase f.

6 If the net external phase-shift parameter, m, is made smaller, f is increased. For a typical engine, m is probably near 2. If the diffuser is a sudden area change at the rear face of the compressor, $m=1$. If circumferential velocity were suppressed in the inlet flow, m might also decrease by 1. A value of $m=0$ may be theoretically possible, if circumferential velocity is suppressed in both entrance and exit flows.

7 Guide vanes have litte effect on f in multistage compressors.

Comparison with Day and Cumpsty's Data. The foregoing results may be compared with the propagation speed data of Day and Cumpsty [2]. Table 1, in the first 5 columns, collects some of their results for various designs, number of stages, and number of stall cells. Of single-cell cases ($n=1$), only the full-span results are included, because the present paper assumes full-span stall, in effect. Multiple-cell cases are included, but it should be noted that all of them are part-span. Guide vanes have a smaller average incidence than core blades, by about a factor of 2. Therefore relative velocities are lower. As a rough estimate, we will assume τ_v to be the average of equation (48) and $2\Phi k$. In that case

$$\frac{\tau_v^*}{\tau^*} = \frac{1}{2}(1+\cos^2\gamma) \tag{50}$$

For the experiments [2] the blade chord is 17.8 mm, and the mean diameter is about 320 mm. The spacing between rows is about one chord width. In that case, if inertia were the only source of lag, we would expect $k=2$. There appears to be a fairly long straight section before the diffuser, and so one

would expect $m=2$. Equation (49) shows that k and m enter in the ratio, k/m. The last two columns of numbers are the theoretical predictions of equation (49) for two values of k/m, the first being for the expected $k/m=1$ ($k=2$, $m=2$), and the second for $k/m=2$. The latter would apply if k were 4 instead of 2 owing to separation hysteresis, or perhaps if the exit acted like an orifice so that $m=1$ instead of 2. The former would be a more likely combination ($m=2$, $k=4$).

Comparing the theoretical and experimental columns, it is clear that equation (49) gives all the proper trends of f with γ, N, and n. We should keep in mind that the theory does not contemplate the part-span stall patterns found experimentally for multiple zones, so agreement for n different from 1 is perhaps fortuitous. The theory probably does not apply well to single-stage situations. Therefore, the most appropriate comparisons are for $n=1$, $N=2$, 3, 4. These cases are enclosed in boxes in the Table, for emphasis.

Table 1 clearly indicates that $k/m=2$ is the best choice for agreement, and the agreement could hardly be closer, for intermediate and high-Φ_d builds. For low Φ_d, full agreement would require a somewhat higher value of k/m, about 3 instead of 2. Perhaps the higher stagger angle causes more hysteresis due to separation.

In the low-Φ_d experiments, a reduced spacing gave a substantially lower speed. In that case, we would expect to reduce the factor k to account for the smaller mass of fluid undergoing oscillation. Because spacing was originally one-chord length, it seems reasonable to reduce k by a factor of 2. Indeed, Table 1 shows that $k/m=1$ gives a prediction having the same relation to experiment for reduced spacing as $k/m=2$ had for the wider spacing. Also, it was mentioned that $k/m=3$ gives exact agreement with experiment for the wider spacing; $k/m=1.5$ gives exact agreement for reduced spacing. Thus, we may add spacing to the list of compressor parameters whose influence on propagation speed is well predicted by equation (49).

Finally, we should note that Cumpsty and Day [10] have derived an equation for propagation speed based on a consideration of pressure jumps across the boundaries of deep-stall zones, together with certain observations of compressor test results. Their equation also predicts the correct trend with number of stages.

Concluding Remarks

The present analyis shows that rotating stall can be considered an eigenfunction of a compressor-inlet-diffuser system if a single lag process occurs in the generation of force by a blade passage, and, at least for weak amplitude, if there is a flat total-to-static pressure rise characteristic in the neighborhood of the average flow coefficient set by the throttle.

The predicted propagation speed depends on various features of the compressor, and follows very closely the trends of experimental observations as those features are changed. The lag processes originating in the compressor (k), and those originating outside the compressor in the entrance duct and the diffuser (m) require more study from a fundamental point of view.

The present analysis, being based on small perturbations, has limited value. First, actual perturbations in deep stall are not small, nor are amplitudes arbitrary. Therefore, there is little guidance from the present analysis as to how compressor parameter changes might help to control or eliminate the phenomenon. However, the results of the present analysis perhaps do give encouragement for the study of finite amplitude oscillations using similar physical assumptions.

Parts II and III of this study report such extensions. In Part II, we keep the restriction to a flat characteristic, but allow the amplitude to be finite. Results will include a measure of how the mean performance is affected by the existence of rotating stall, as well as certain interesting velocity and pressure profiles. In Part III, we attempt to relate rotating stall to the complete characteristic curve. Results include an indication of when the "blockage" model [3] applies, and also predict that rotating stall becomes impossible beyond some value of flow coefficient, probably indicating the onset of stall recovery.

References

1 Greitzer, E. M., "Review—Axial Compressor Stall Phenomena," ASME *Journal of Fluids Engineering*, Vol. 102, June 1980, pp. 134–151.

2 Day, I. J., and Cumpsty, N. A., "The Measurement and Interpretation of Flow Within Rotating Stall Cells in Axial Compressors," *Journal of Mechanical Engineering Sciences*, Vol. 20, 1978, pp. 101–114.

3 Day, I. J., Grietzer, E. M., and Cumpsty, N. A., "Prediction of Compressor Performance in Rotating Stall," ASME JOURNAL OF ENGINEERING FOR POWER, Vol. 100, Jan. 1978, pp. 1–14.

4 Emmons, H. W., Pearson, C. E., and Grant, H. P., "Compressor Surge and Stall Propagation," ASME *Transactions*, Vol. 27, Apr. 1955, pp. 455–469.

5 Graham, R. M., and Guentert, E. C., "Compressor Stall and Blade Vibration," Chapter XI in *Aerodynamic Design of Axial-Flow Compressors*, NASA SP-36, 1965.

6 Sears, W. R., "Rotating Stall in Axial-Flow Compressors," *Zeitschrift fur Angewandte Mathematik und Physik*, Vol. 6, No. 6, 1955, p. 429–455.

7 Marble, F. E., "Propagation of Stall in a Compressor Blade Row," *Journal of the Aeronautical Sciences*, Vol. 22, 1955, pp. 541–554.

8 Stenning, A. H., Kriebel, A. R., and Montgomery, S. R., "Stall Propagation in Axial-Flow Compressors," NACA TN 3580, 1956.

9 Takata, H., and Nagano, S., "Nonlinear Analysis of Rotating Stall," ASME JOURNAL OF ENGINERING FOR POWER, Oct. 1972, pp. 279–293.

10 Cumpsty, N. A., and Grietzer, E. M., "A Simple Model for Compressor Stall-Cell Propagation," ASME JOURNAL OF ENGINEERING FOR POWER, Vol. 104, Jan. 1982, pp. 170–176.

11 Stoker, J. J., *Nonlinear Vibrations*, ch. 5, Interscience, New York, 1950.

12 Moore, F. K., "Lift Hysteresis at Stall as an Unsteady Boundary-Layer Phenomenon," NACA TN 3571, 1951.